Sensors & Transducers, Vol. 249, Issue 2, February 2021, pp. 36-44

Sensors & Transducers
Published by IFSA Publishing, S. L., 2021
http://www.sensorsportal.com

Image Enhancement in the LIP Framework and Noise Reduction with Deep Convolutional Neural Networks to Produce High Quality Images from Low Light Acquisitions

[1,*] Maxime CARRE and [2] Michel JOURLIN
[1] NT2I Company, 10 rue Jean Servanton, 42000 Saint-Etienne, France
[2] Hubert Curien Laboratory, 18 rue du Pr Lauras, 42000 Saint-Etienne, France
E-mail: m.carre@nt2i.fr

Received: 15 October 2020 /Accepted: 31 January 2021 /Published: 28 February 2021

Abstract: The LIP (Logarithmic Image Processing) model is recognized as an efficient framework to process images acquired in transmitted and reflected light, and to take into account the human visual system. Several image enhancement algorithms have been developed in the LIP framework. Some of them exploit an important property of the LIP model consisting in simulating exposure time variations. Applied to very low light images, our LIP algorithms enhance not only the signal, but also the noise and lead to quantized grey levels. Noise reduction based on Deep Convolutional Neural Networks is performed on these enhanced noisy images. The combination of LIP enhancement and DCNN denoising transforms low light images into well-balanced images with low noise level. In addition to classical PSNR evaluation, we propose an estimation of image noise based on LIP contrasts computed at a local scale. The use of LIP contrast results in a noise evaluation consistent with human vision.

Keywords: LIP model, Exposure time simulation, Image enhancement, Low light images, Noise reduction, Deep convolutional neural networks.

1. Introduction

This paper is an extended version of work presented in [1].

For the reader not familiar with the LIP framework, we propose the following references: [2-4], and more recently an overview book [6]. The LIP Model was first dedicated to images acquired in transmission (Fig. 1) when the observed object is located between the source and the sensor and its opacity and thickness may be variable. Such a situation is very common in the biomedical field (microscopy, tomography, scanner…).

We will see later why the Model is also useful for images acquired in reflection. The applications described in this paper are mainly about reflected light acquisition, but the proposed solution can be used in both configurations: transmitted and reflected light imaging.

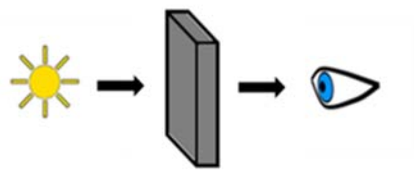

Fig. 1. Image acquired in transmittance: the source, the semi-transparent obstacle, and the sensor.

2. Basis of the LIP Model

Let us define D as the spatial domain. If f is an image defined on D with values in the grey scale $[0, M[$, the transmittance $T_{f(x)}$of f at $x \in D$ is the ratio of the transmitted flux at x by the incoming flux (intensity of the source):

$$T_{f(x)} = \frac{I_t(x)}{I_i(x)} \qquad (1)$$

Note that within the LIP model, the grey scale is inverted: 0 corresponds to the "white" extremity of the grey scale, which means to the source intensity, i.e. when no obstacle (object) is placed between the source and the sensor. M corresponds to the "black" extremity.

In a mathematical formulation, the transmittance $T_{f(x)}$ is the probability, for a particle of the source incident at x, to pass through the obstacle that is to say to be seen by the sensor.

The addition $f \triangle\!\!\!\!+ g$ of two images f and g is associated to the superposition of the objects generating f and g (Fig. 2).

Fig. 2. Addition of two images.

In this case, the transmittance law can be written:

$$T_{f \triangle\!\!\!\!+ g} = T_f . T_g \qquad (2)$$

A link has been established ([4]) between the grey level $f(x)$ and the transmittance $T_{f(x)}$ according to:

$$T_{f(x)} = 1 - \frac{f(x)}{M} \qquad (3)$$

By replacing such transmittances values in (2), the following addition formula is obtained:

$$f \triangle\!\!\!\!+ g = f + g - \frac{f . g}{M} \qquad (4)$$

From (4), the product $\lambda \triangle\!\!\!\!\times f$ by a real number λ is deducted:

$$\lambda \triangle\!\!\!\!\times f = M - M(1 - \frac{f}{M})^{\lambda} \qquad (5)$$

Such laws (4) and (5) possess interesting properties: at a physical level, they refer to the Transmittance Law and at a mathematical level, they give a structure of Vector Space to the set $I(D, [0, M[)$ of images defined on D with values in the grey scale $[0, M[$. This is due, in particular, to the possibility to define a subtraction operator $\triangle\!\!\!\!-$:

$$f \triangle\!\!\!\!- g = \frac{f - g}{1 - \frac{g}{M}} \qquad (6)$$

Note that when f is greater (darker) than g for each point x of D, $f \triangle\!\!\!\!- g$ takes its values in the grey scale and is then an image.

Plenty of new concepts and tools have been defined in the LIP framework, for example new notions of contrast (Logarithmic Additive Contrast, Logarithmic Multiplicative Contrast) and new metric tools (cf. [5] and [6] for more details and various applications).

Considering two points x and y of D and a grey level function f, the following notions of contrast are commonly used:

- The simplest one consists of computing the absolute value $|f(x) - f(y)|$ of the difference between $f(x)$ and $f(y)$.

- Knowing that the Human Visual System is not linear but of logarithmic nature, such a contrast is not adapted to model a Human Visual interpretation of an image. To give a higher weight to contrasts between dark points, a "physician" approach has been introduced, the Michelson contrast. If R is a subset of D, this contrast of f inside R, $C_R^{Mi}(f)$ is estimated as:

$$\frac{Max_{x \in R}\left(f(x)\right) - Min_{x \in R}\left(f(x)\right)}{Max_{x \in R}\left(f(x)\right) + Min_{x \in R}\left(f(x)\right)} \qquad (7)$$

If the region R is restricted to a pair of neighboring points (x, y), $C_{(x,y)}^{Mi}(f)$ becomes:

$$\begin{cases} \frac{|f(x) - f(y)|}{f(x) + f(y)} \text{ if } f(x) \neq 0 \text{ or } f(y) \neq 0 \\ 0 \text{ if } f(x) = f(y) = 0 \end{cases} \qquad (8)$$

Quotient in Formula (8) may be interpreted as the coefficient of variation of the pair $(f(x), f(y))$, i.e. the standard deviation divided by the mean value.

Inside the LIP framework, a similar notion, namely the Logarithmic Additive Contrast (LAC) between $f(x)$ and $f(y)$. $C_{(x,y)}^{\triangle\!\!\!\!+}(f)$ or $C_{(x,y)}^{\triangle\!\!\!\!+}$ when no confusion is possible, is obtained according to:

$$Max\left(f(x), f(y)\right) \triangle\!\!\!\!- Min\left(f(x), f(y)\right) = \frac{|f(x) - f(y)|}{1 - \frac{Min(f(x), f(y))}{M}} \qquad (9)$$

Remark: If $f(x)$ is noted f, and $f(y)$ becomes $f + \delta f$, the definition of Formula (9) shows that the LAC is expressed as:

$$M \frac{\delta f}{M - f} = MW \qquad (10)$$

This result is comparable to the equality established in [3] between the Weber constant W and the quotient $\delta f\ /(\ M-f)$. Thus, we can assert that the LAC follows the Weber - Fechner law. This point justifies the use of the Logarithmic Additive Contrast to evaluate the visual quality of a denoising step.

To complete the previous remark, Brailean ([7]) demonstrated that the Model is consistent with Human Vision, which means that the LIP tools are successfully applicable to images acquired in reflection, particularly when we want to interpret those images as a human eye would do.

Physical interpretation of Formula (9): the LAC between two grey levels appears obviously as the grey level which must be added (i.e., superposed in transmitted light) to the brightest in order to obtain the darkest one.

The Michelson's contrast is explicitly linked to the LAC one according to the Formula (cf. [6]):

$$\begin{aligned} &M.C^{Mi}(f(x),f(x)+2k) \\ &=C^{\triangle\!\!\!+}(M-f(x),M-f(x)-k) \end{aligned} \tag{11}$$

Such a formula assigns a physical meaning to the Michelson's contrast. Moreover, the difference between the two considered grey levels must be doubled for Michelson: this explains why in our first experimentations the LAC appeared more sensitive than Michelson.

A useful application of the LAC consists of defining it locally. If N is a neighborhood of x, it is possible to compute the value of $C^{\triangle\!\!\!+}_{(x,y)}$ for each y of N and then to take the maximum or the average of these values:

$$\max_{y\in N} C^{\triangle\!\!\!+}_{(x,y)} \text{ or } \frac{1}{n}\sum_{y_i\in N} C^{\triangle\!\!\!+}_{(x,y_i)} \tag{12}$$

This application can be used for contour detection purposes, or in the present work, for noise evaluation. By computing the average value of every local contrasts, we get an estimation of the global noise level inside the image.

3. Image Enhancement in the LIP Framework

One of the most significant properties of the LIP model consists of simulating exposure time variations ([8]). Indeed, it has been demonstrated that LIP addition and subtraction can be used to simulate variations of source intensity or sensor's sensitivity.

Physically, a LIP addition of an image by a constant value is equivalent to placing a homogenous absorbing medium (in addition to the observed object) between the source and the sensor and thus reducing the incoming intensity of the source. It may be interpreted also as a reduction of sensor's sensitivity. The exposure time is an evident camera setting able to modify this sensitivity.

In both interpretations, the effect will be the same on the resulting image: it will be darkened compared to the image generated without this added absorbing medium.

At the opposite, a LIP subtraction of an image by a constant value is equivalent to remove a homogenous part of the observed object. In analogy with the LIP addition, this removal increases the source intensity or the sensor's sensitivity. Then the resulting image will be a brightened version of the image acquired without this removal (Fig. 3).

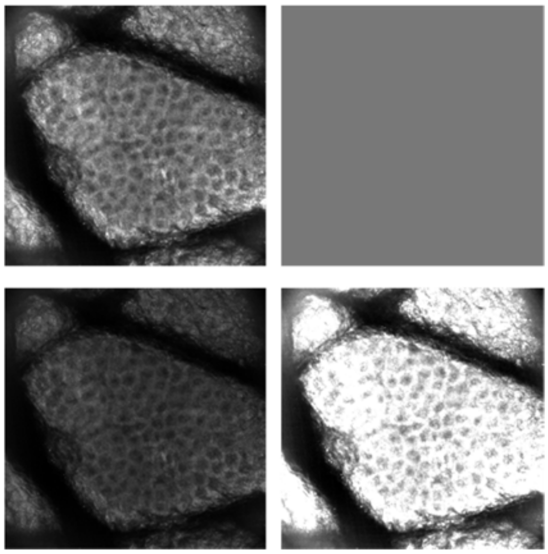

Fig. 3. LIP addition and subtraction. Top left: image acquired in transmitted light, top right: uniform image with grey level 128, bottom left: LIP addition of the original image and the uniform image, bottom right: LIP subtraction of the original image by the uniform image.

These principles are defined in a transmitted light configuration. In a reflected light configuration, it has been demonstrated [8] that the simulation of sensor sensitivity, exposure time for instance, by LIP addition/subtraction is also well adapted (Fig. 4).

Let us return in transmitted light imaging to understand the effect of a LIP multiplication of an image.

Physically, the LIP product of an image by a scalar λ is a homothety which equates to modify the thickness of the observed object. Using λ > 1 permits to increase the thickness while using λ < 1 decreases it. Obviously, a reduced thickness increases the brightness of the resulted image (the incoming flux is less filtered) and a larger thickness darkens the resulted image (the incoming flux is more filtered).

In reflected light conditions, this operation has no evident interpretation. But the non-linearity of the LIP multiplication and its isomorphism property (it applies the grey scale [0,255] on itself: the output values cannot exceed the grey level range) can be efficient for image enhancement (Fig. 5). It can be used as a tone mapping operation to improve the display of high dynamic images.

Fig. 4. Simulation of exposure time variation. Left: image acquired at 10 ms, right: simulation of 100 ms exposition applied to the image acquired at 10 ms.

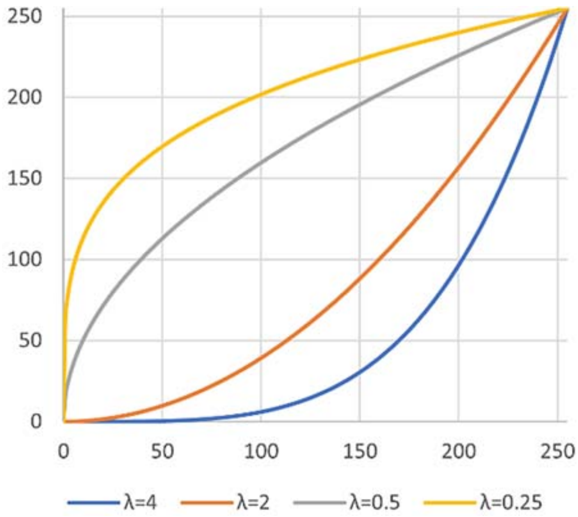

Fig. 5. Look Up Tables between input and output grey levels for multiple λ values.

Some algorithms based on LIP multiplication have been developed. They aim at computing λ automatically to optimize an image parameter, for example, maximizing the standard deviation of the image histogram ([6], chapter IV) or stabilizing the brightness to a specific value.

An example of image enhancement using LIP multiplication is proposed in Fig. 6, for a color image. To process color images, the same operations are applied on each channel R, G, B to guarantee the conservation of real colors (same λ for each channel). Color images can also be processed with the LIPC model [9] considering more specifically human vision.

Another LIP enhancement algorithm directed to local tone mapping has been developed ([10]) using LIP subtraction. The principle of this algorithm is to simulate local variations of exposure time and aims at stabilizing spatially the brightness of the image to a minimum value. Dark regions are enhanced while bright regions correctly balanced are kept untouched. The local brightness is modelized using a Bilateral Filtering. In this filtering, the classical grey level distance has been replaced by a LIP additive contrast producing a constant filtering, independent of lighting variations.

The use of LIP subtraction, simulating exposure time variation aims at producing a realistic image enhancement. An example is proposed in Fig. 7.

Fig. 6. LIP multiplication. Left: night street image, right: image enhanced by LIP ⨻ to maintain an average of 100 (grey level) on the luminance plane.

Fig. 7. Spatial stabilization. Left: image of a street with a strong shadow, right: image enhanced with local exposition variations.

4. Problem: Noise and Quantization

Let us remember that whatever the enhancement method, image noise is amplified as well as image information. Strong noise can be a discomfort for a human observer and source of difficulties for many image analysis algorithms.

In particular, such a problem arises when applying the exposure time simulation to low-light images in order to enhance them.

On Fig. 9, we apply on a sequence of images acquired at different exposure times (Fig. 8) a brightness stabilization algorithm based on LIP exposure time simulation ([10]). In this example, each image is stabilized to a reference brightness corresponding to the image acquired with the higher exposure time, here 50 ms. Obviously, the noise level increases as the exposure time decreases.

Such a problem damages the quality of the enhanced image and necessitates the application of a noise filtering more or less adapted to the considered images.

Another issue concerns the quantization of the grey level scale. Since the original dark image presents a compressed histogram, our enhancement leads to a quantized histogram (Fig. 9). In the case of strong exposure time correction, this quantization can be visible by a human observer.

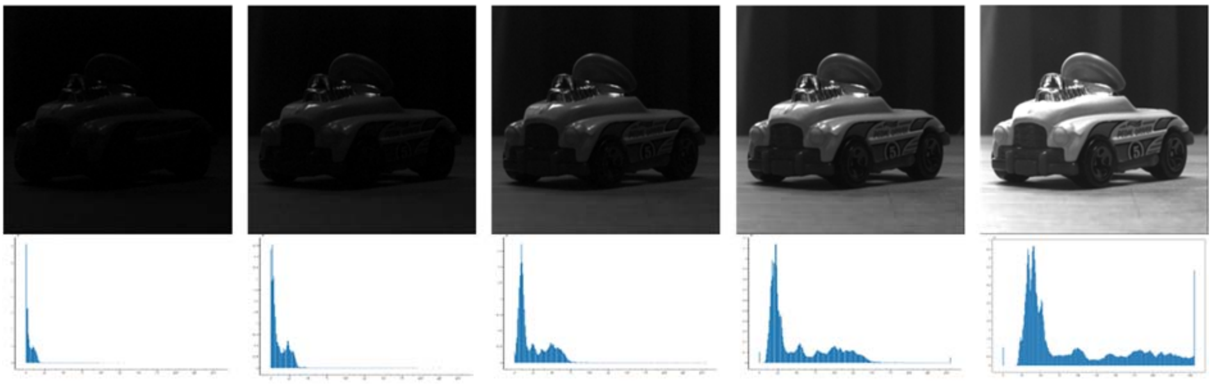

Fig. 8. Images acquired at different exposure times, from left to right: 0.75 ms, 2.22 ms, 6.67 ms, 20 ms, 50 ms.

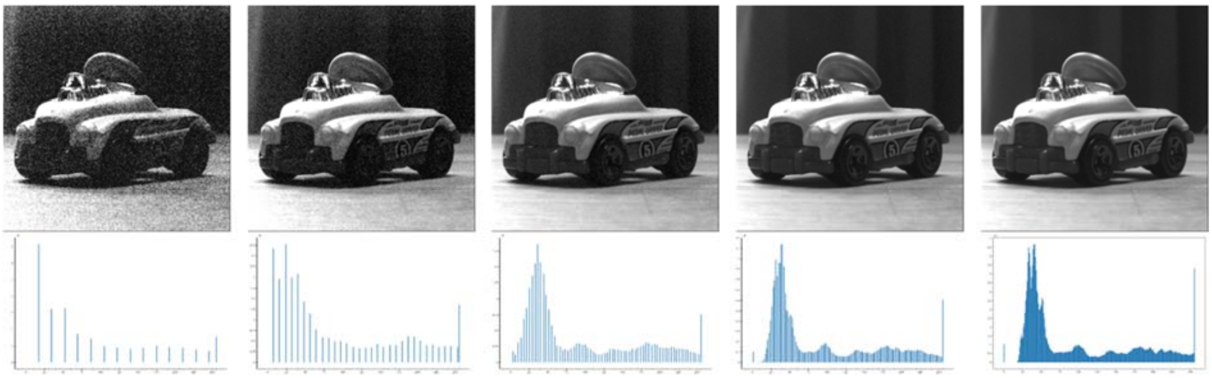

Fig. 9. LIP stabilization applied on Fig. 1 images.

5. Proposed Solution

To overcome those drawbacks, we decided to apply a Deep Learning approach, according to [11]. This approach consists of restoring noisy images by training a convolutional neural network. The proposed network is based on a U-network shape ([12]) and the particularity of [11] lies in the use of only corrupted couples of images in the training phase, instead of classical couples constituted of a noisy image and a clean one.

In our situation, this particularity greatly facilitates the preparation of images databases required in machine learning methods. Generating thousands of noisy/clean images would require an acquisition system able to switch quickly between two exposure times (a low exposure time for the noisy image, and a higher one for the clean target). Creating sequences of noisy images acquired in the same conditions is much easier and makes the solution adaptable to many acquisition systems.

In order to process enhanced images presenting different noise intensities as described in Fig. 9, we train the network with images acquired under different brightness conditions and variable exposure times.

6. Results

Fig. 10 and Fig. 10 (b) show the application of the trained network on the images of Fig. 9. In each situation, the noise has been significantly reduced. This visual estimation is confirmed by Table 1, presenting the evolution of PSNR computed for each exposure time on images processed with LIP enhancement only and processed with the combination of LIP enhancement and DCNN (Deep Convolutional Neural Networks) denoising.

Table 1. PSNR according to exposure level.

Expo. (ms)	**0.75**	**2.22**	**6.67**	**20**	**50**
LIP	19.3	23.4	28.8	31.5	clean
LIP denois.	25.4	27.2	33.3	37.6	clean

In addition to the PSNR evaluation, we propose to estimate the noise level of images using LIP tools. As explained above in Section 2, the average value of LIP contrasts computed in each pixel with its neighboring points represents an estimation of the intensity of image noise. In comparison to classical grey levels distance, using LIP additive contrast aims at interpreting grey levels closer to human sensitivity.

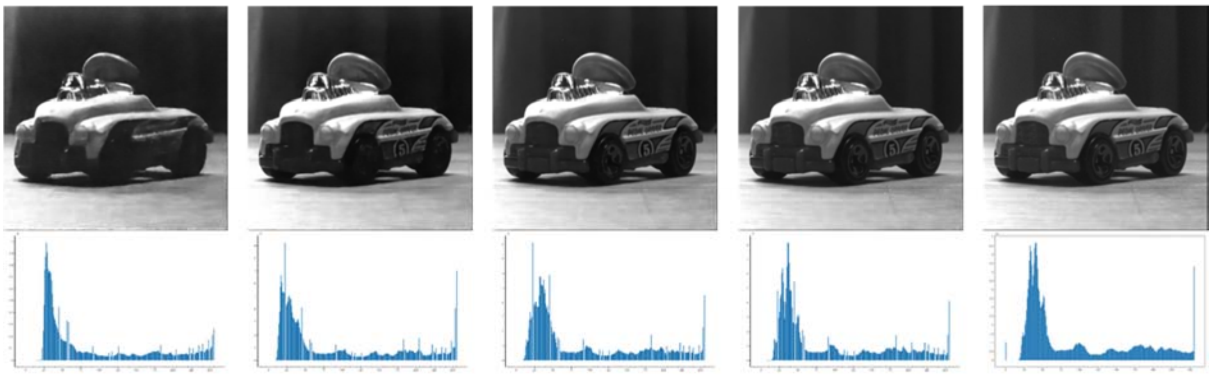

Fig. 10. Noise and quantization correction on Fig. 2 images.

0.75 ms 2.22 ms 6.67 ms 20 ms 50 ms

Fig. 10 (b). Top: Zoom on images acquired at different exposure times processed with LIP stabilization, bottom: zoom on images acquired at different exposure times processed with LIP stabilization and noise reduction.

Table 2 presents LIP noise estimations based on this average of LIP contrasts computed at a local scale.

Unlike the PSNR evaluation comparing images to a clean reference, each image gets an absolute noise level (without reference). That is why a noise level is also proposed for the clean target in Table 2.

Table 2. Average LIP contrast according to exposure level, values in the grey level scale [0, 255].

Expo. (ms)	**0.75**	**2.22**	**6.67**	**20**	**50**
LIP	65.5	58.5	29.7	14.6	10.5
LIP denois.	7.2	8.8	8.4	7.7	7.4

Each denoised image gets a noise intensity inferior to 10 grey levels, while original images get values between 65.5 and 10.5.

It is interesting to note that the denoised version of the originally noisiest image (0.75 ms exposure time) gets a lower noise value than the clean target. This is due to the loss of details of this extreme case, resulting in a “simplified” image. Some information could not be recovered from the original very dark image (Fig. 10 (b)).

We can notice also that the image corresponding to the clean target (without the application of the denoising step) gets a noise level superior to all the denoised ones. By looking closely to its details, it can be explained by the “image grain”: even the clean target gets a minimum noise level, which can be reduced by the denoising network.

Visually, starting from the 6.67 ms exposure time, the resulting images are very close to the clean target despite a slightly blurred rendering. This blur effect is a frequent issue in denoising problematics (see zoomed images in Fig. 10 (b)).

In our case, the benefits of the network are twofold: as expected the noisy signal is cleaner, and in addition the quantization of the signal is corrected. Indeed, due to the last layer of the neural network presenting a linear activation, the output signals get continuous values, while every trained one were quantized. This point appears clearly by comparing the histograms of Fig. 9 and Fig. 10.

7. Applications

The proposed solution, LIP brightness stabilization and noise reduction with DCNN, can be directly applied to color images by learning RGB noisy images. An example is shown on Fig. 11 and Fig. 11 (b).

The adaptation of the network to different noise intensities allows its application to images enhanced by another LIP algorithm performing brightness spatial stabilization ([10]), described in Section 3. This algorithm consists of simulating local variations of exposure time to process high dynamic images. The brightness is locally adjusted to enhance only the dark areas. This local correction leads to different noise intensities within a single image. Since the network has been trained under different brightness conditions, its application in this situation is well adapted.

An example is proposed in Fig. 12 and Fig. 12 (b). Regions initially bright and with a very low level of noise are almost untouched: the brightness is not modified but low noise can be slightly corrected as described in Section 6. Dark regions are much more modified: the brightness is enhanced, increasing the noise, which is significantly reduced by the denoising network. Finally, the resulting image is well balanced in every region with low levels of noise. A limit of the solution is related to too dark areas in which information cannot be retrieved.

Fig. 11. Application on a color image. From left to right: low exposure acquisition (2 ms), LIP stabilization applied on the low exposure image, noise reduction applied on the enhanced image, high exposure acquisition (clean target, 50 ms).

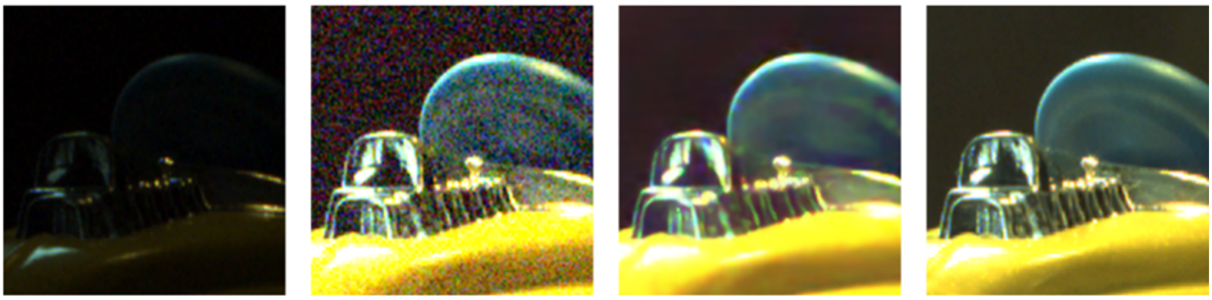

Fig. 11 (b). Zoom on Fig. 11.

Fig. 12. Brightness spatial stabilization. From left to right, low exposure acquisition (5 ms), higher exposure exposition (50 ms) leading to burned areas, LIP local stabilization applied on the low exposure image, noise reduction applied on the enhanced image.

Fig. 12 (b). Zoom on Fig. 12.

8. Discussion

In the present paper, we propose a novel solution that focuses on enhancing very low-light images in the LIP framework. By adding a denoising process based on DCNN to LIP enhancement algorithms, very dark images or complex images with dark and bright regions can be corrected to stabilize the brightness and reduce drastically the noise level.

Using some optimizations [13], the denoising network, based on a U-Net architecture can be run in real time, as well as most of the LIP enhancement algorithms.

Other low light imaging applications can be processed by the proposed solution. For example, image acquisition of moving objects using standard exposure times lead to blur results. This is commonly the case for sports meetings, traffic surveillance and for industrial control when objects are transported by means of a conveyor. In such situations, the solution to acquire clear images consists of drastically reducing the exposure time, which produces low-light images.

We have already mentioned ([14]) the ability of the LIP Model to enhance such images. Nevertheless, at this time we had not applied the denoising step.

We plan also to develop the combination LIP tone mapping algorithm and DCNN denoising to compare HDR (High Dynamic Range) image generated from multiple exposure images and HDR image generated from a single exposure image enhanced and denoised.

References

[1]. M. Carre, M. Jourlin, Exposure Time Simulation thanks to the LIP (Logarithmic Image Processing) Model with Noise Reduction by Deep Convolutional Neural Networks, in *Proceedings of the 2nd International Conference on Advances in Signal Processing and Artificial Intelligence (ASPAI'2020)*, 2020, pp. 46-49.

[2]. M. Jourlin, J.-C. Pinoli, Logarithmic Image Processing, *Acta Stereologica*, Vol. 6, 1987, pp. 651-656.

[3]. M. Jourlin, J.-C. Pinoli, A model for Logarithmic Image Processing, *Journal of Microscopy*, Vol. 149, Issue 1, 1988, pp. 21-35.

[4]. M. Jourlin, J.-C. Pinoli, Logarithmic Image Processing: The mathematical and physical framework for the representation and processing of transmitted images, *Advances in Imaging and Electron Physics*, Vol. 115, 2001, pp. 129-196.

[5]. M. Jourlin, M. Carre, J. Breugnot, M. Bouabdellah, Logarithmic image processing: additive contrast, multiplicative contrast, and associated metrics, *Advances in Imaging and Electron Physics*, Vol. 171, 2012, pp. 357-406.

[6]. M. Jourlin, Logarithmic Image Processing: Theory and Applications, *Advances in Imaging and Electron Physics*, Vol. 195, 2016, pp. 2-259.

[7]. J. Brailean, B. Sullivan, C. Chen, M. Giger, Evaluating the EM algorithm for image processing using a human visual fidelity criterion, in *Proceedings of the International Conference on Acoustics, Speech, and Signal Processing (ICASSP),* Vol. 4, 1991, pp. 2957–2960.

[8]. M. Carre, M. Jourlin, LIP operators: Simulating exposure variations to perform algorithms independent of lighting conditions, in *Proceedings of the International Conference on Multimedia Computing and Systems (ICMCS)*, 2014, pp. 122–126.

[9]. M. Jourlin, J. Breugnot, F. Itthirad, M. Bouabdellah, B. Closs, Logarithmic Image Processing for Color Images, *Advances in Imaging and Electron Physics*, Vol. 168, 2011, pp. 65-108.

[10]. M. Carre, M. Jourlin, Brightness spatial stabilization in the LIP framework, in *Proceedings of the 14th International Congress for Stereology and Image Analysis (ICSIA)*, *Acta Stereologica,* 2015.

[11]. J. Lehtinen, J. Munkberg, J. Hasselgren, S. Laine, T. Karras, M. Aittala, T. Aila, Noise2Noise: Learning Image Restoration without CleanData, in *Proceedings of the 35th International Conference on Machine Learning,* Stockholm, Sweden, PMLR 80, 2018, pp. 2965-2974.

[12]. O. Ronneberger, P. Fischer, T. Brox, U-net: Convolutional networks for biomedical image segmentation, *Medical Image Computing and Computer-Assisted Intervention (MICCAI*), Vol. 9351, 2015, pp. 234–241.

[13]. D. Brittain, Creating performant DL models for use in client applications, in *Proceedings of the GPU Technology Conference (GTC 2020)*, 2020.

[14]. V. Deshayes, P. Guilbert, M. Jourlin, How simulating exposure time variations in the LIP model. Application: moving objects acquisition, in *Proceedings of the 14th International Congress for Stereology and Image Analysis (ICSIA)*, *Acta Stereologica,* 2015.

Universal Sensors and Transducers Interface (USTI-EXT) Series of IC for Automotive Applications
• Precision measurements of frequency-time parameters of sensor outputs
• rpm measurements
• Cx, Rx and Resistive Bridges measurements
• Extended temperature range from -55 °C to +150 °C
• I²C, SPI and RS232
USTI-EXT
IFSA
http://www.sensorsportal.com/HTML/E-SHOP/e-shop_4.htm